February 2007

Somatic excision demonstrates that c-Jun induces cellular migration and invasion through induction of stem cell factor

Sanjay Katiyar
Thomas Jefferson University

Xuanmao Jiao
Thomas Jefferson University

Erwin Wagner
Research Institute of Molecular Pathology, Vienna, Austria

Michael P. Lisanti
Thomas Jefferson University

Richard G. Pestell
Thomas Jefferson University, Cecilia.Deemer@kimmelcancercenter.org

MOLECULAR AND CELLULAR BIOLOGY, Feb. 2007, p. 1356–1369 Vol. 27, No. 4
0270-7306/07/$08.00+0 doi:10.1128/MCB.01061-06

Somatic Excision Demonstrates that c-Jun Induces Cellular Migration and Invasion through Induction of Stem Cell Factor▽†

Sanjay Katiyar,[1] Xuanmao Jiao,[1] Erwin Wagner,[2] Michael P. Lisanti,[1] and Richard G. Pestell[1]*

Kimmel Cancer Center, Departments of Cancer Biology and Medical Oncology, Thomas Jefferson University, 233 South 10th Street, Philadelphia, Pennsylvania 19107,[1] and Research Institute of Molecular Pathology, Dr Bohr-Gasse 7, Vienna A-1030, Austria[2]

Received 13 June 2006/Returned for modification 14 July 2006/Accepted 18 November 2006

Cancer cells arise through sequential acquisition of mutations in tumor suppressors and oncogenes. c-Jun, a critical component of the AP-1 complex, is frequently overexpressed in diverse tumor types and has been implicated in promoting cellular proliferation, migration, and angiogenesis. Functional analysis of candidate genetic targets using germ line deletion in murine models can be compromised through compensatory mechanisms. As germ line deletion of c-*jun* induces embryonic lethality, somatic deletion of the c-*jun* gene was conducted using floxed c-*jun* (c-*jun*$^{f/f}$) conditional knockout mice. c-*jun*-deleted cells showed increased cellular adhesion, stress fiber formation, and reduced cellular migration. The reduced migratory velocity and migratory directionality was rescued by either c-Jun reintroduction or addition of secreted factors from wild-type cells. An unbiased analysis of cytokines and growth factors, differentially expressed and showing loss of secretion upon c-*jun* deletion, identified stem cell factor (SCF) as a c-Jun target gene. Immunoneutralizing antibody to SCF reduced migration of wild-type cells. SCF addition rescued the defect in cellular adhesion, cellular velocity, directional migration, transwell migration, and cellular invasion of c-*jun*$^{-/-}$ cells. c-Jun induced SCF protein, mRNA, and promoter activity. Induction of the *SCF* promoter required the c-Jun DNA-binding domain. c-Jun bound to the *SCF* promoter in chromatin immunoprecipitation assays. Mutation of the c-Jun binding site abolished c-Jun-mediated induction of the *SCF* promoter. These studies demonstrate an essential role of c-Jun in cellular migration through induction of SCF.

The c-*jun* proto-oncogene encodes a prototypical member of the AP-1 transcription factor family. c-Jun heterodimerizes with members of the Jun/Fos and MaF/Nr1 families through a leucine zipper motif. AP-1 proteins, in turn, regulate transcriptional activity of downstream target genes or interact directly to influence transcription through association with other transcription factors (13, 23, 28, 39). Phosphorylation of the c-Jun N-terminal kinase (JNK) subgroup of mitogen-activated protein (MAP) kinases plays a key role in responding to diverse stress signals (28). JNK activation has been linked to both the inhibition and induction of cellular apoptosis and to the regulation of cellular migration (26, 68, 69).

The migration of cells plays a critical role in a broad variety of biological processes including cellular development, tissue repair, and metastasis of tumors (29, 34, 42). Initiation of cellular migration requires cell substratum adhesion interaction and the sequential generation of membrane protrusions (36). Actin polymerization provides both protrusive activity and directionality of cellular movement. New adhesive sites are sequentially established in the extended membranes. Motile cells constantly remodel transient adhesions at the leading edges (43). In fibroblasts, focal complexes form which mature into focal adhesions. Remodeling of these focal adhesions is important, as cell motility is a dynamic balance between contractual forces driving the cell body forward and detachment of the posterior edge of the cell from its substratum.

Cellular migration is induced by a variety of growth factors and cytokines. Stem cell factor (SCF), and its receptor Kit, play pivotal roles in cellular migration as well as differentiation, proliferation, and migration (74). SCF exists as a secreted soluble form and as a membrane-bound glycoprotein (15, 73). Complete absence of SCF in the mouse is embryonic lethal (15), and SCF binding to Kit induces cellular migration of diverse cell types including neural stem cells and endothelial cells (33). SCF directly activates microvascular endothelial cells to promote tumor angiogenesis (55). Intracellular kinases are activated consequent upon ligand-induced dimerization and transphosphorylation of Kit, a type III receptor protein-tyrosine kinase (70). The relative importance of SCF-induced JNK, Akt, and extracellular signal-regulated kinase (ERK) activity to cellular migration remains to be fully understood.

c-*jun*$^{-/-}$ mice die in gestation from cardiovascular and hepatic defects (12). Therefore, to examine the role of c-Jun in cellular adhesion, migration, and directional persistence, transgenic mice carrying floxed c-*jun* alleles (c-*jun*$^{f/f}$) in which the gene was flanked by *loxP* sites were used herein. Acute excision of c-*jun* using Cre recombinase identified a key role for c-Jun in cellular adhesion. Within 48 h of c-*jun* excision, c-*jun*$^{-/-}$ fibroblasts were round and flat and demonstrated greater cellular spreading. Cellular adhesion was enhanced in c-*jun*$^{-/-}$ murine embryonic fibroblasts (MEFs), associated with increased stress fiber formation and reduced migration into a wound. c-Jun induced both the velocity of cellular migration as well as directional persistence. The reduced persistence of migratory directionality of c-*jun*$^{-/-}$ cells was reversed by the

* Corresponding author. Mailing address: The Kimmel Cancer Center, Departments of Cancer Biology and Medical Oncology, Thomas Jefferson University, 233 South 10th St., Philadelphia, PA 19107. Phone: (215) 503-5649. Fax: (215) 503-9334. E-mail: Richard.Pestell@jefferson.edu.

† Supplemental material for this article may be found at http://mcb.asm.org/.

▽ Published ahead of print on 4 December 2006.

TABLE 1. List of oligonucleotide primers used in this study[a]

Gene (purpose)[b]	Orientation	Sequence 5′→3′
SCF promoter cloning	Forward	ATA GGC TAG CAG CAC AGA CTT CCC TCC ACA AAG T
	Reverse	CAT GGA AGC TTT GTG GCG ACT CCG TTT AGC T
c-*jun* genotyping	Forward	CTC ATA CCA GTT CGC ACA GGC GGC
	Reverse	CCG CTA GCA CTC ACG TTG GTA GGC
	Reverse	CAG GGC GTT GTG TCA CTG AGC T
RPL-19 (DNA PCR)	Forward	AAT GCT CGG ATG CCT GAG AA
	Reverse	CTC CAT GAG GAT GCG CTT GT
Cre recombinase	Forward	TGC TCT GTC CGT TTG CCG
	Reverse	ATC GTG TCC AGA CCA GGC
RPL-19 (for RT-PCR)	Forward	CTGAAGGTCAAAGGGAATGTG
	Reverse	GGACAGAGTCTTGATGATCTC
c-*jun* (for RT-PCR)	Forward	AGA GCG GTG CCT ACG GCT ACA GTA A
	Reverse	CGA CGT GAG AAG GTC CGA GTT CTT G
SCF (KL-1, soluble)	Forward	GGAATCCTGTGACTGATAATGT
	Reverse	CAGGGGGTAACATAAATGGT
SCF (KL-2, membrane bound)	Forward	GGA ATC CTG TGA CTG ATA AT
	Reverse	CTA AGG GAG CTG GCT GCA AC
18S rRNA	Forward	AGGAATTCCCAGTAAGTGCG
	Reverse	GCCTCACTAAACCATCCAA
AP-1-like elements (1)	Forward	GCT GGG AAA GGC AAG GAA ATG GAA
	Reverse	TGC AAC TCC TTG CTA GTG CCT ACT
AP-1-like element (2)	Forward	GGC AGT ATG TCC AAG GTT CTG GAT
	Reverse	TCCA TGT TAT AGA TTA AGA AAT AGC CTC AAGT
AP-1 element (3)	Forward	CTT TCT GTG AGA ACA ACC CGC AGT
	Reverse	TCC TTC CTT CTT CCT TCC TCC CTT
Negative (4)	Forward	TTC ATT TGC TGT CTG TCA CCG GG
	Reverse	TGC AGA TAG TCC CAG CAT TGG GTA

[a] Primers used in cloning SCF promoter, PCR, RT-PCR, real-time quantitative RT-PCR analysis (54), and ChIP assays.
[b] Numbers in parentheses refer to AP-1 elements and negative control (see promoter line diagram in Fig. 11).

addition of medium from parental c-*jun*$^{+/+}$ cells. Using an unbiased array-based proteomic approach, subtractive analysis of cytokine and growth factors differentially secreted upon deletion of c-*jun* identified SCF as a cytokine secreted in response to c-Jun. SCF rescued the defective migration of c-*jun*$^{-/-}$ cells, and SCF expression was induced by c-Jun. Together these studies demonstrate a key role for c-Jun in cellular migration through induction of SCF.

MATERIALS AND METHODS

Transgenic mice, expression plasmids, and promoter cloning. Transgenic animals carrying floxed c-*jun* alleles, c-*jun*$^{f/f}$, were previously described (71). All experimental procedures with these mice were approved by the ethics committee of Georgetown and Thomas Jefferson University. Animals were examined for a coital plug to define the day zero of gestation whenever copulation was detected. The MEFs were produced as previously described (1) and cultured following the 3T3 protocol (60).

The expression plasmids encoding adenovirus directing Cre (Ad-Cre) expression or control virus (Ad-Null) were previously described (66). The EcoR1 fragment of the rat c-*jun* DNA (53) was subcloned into a retroviral expression vector, murine stem cell virus-internal ribosomal entry site-green fluorescent protein (MSCV-IRES-GFP), to form MSCV-c-Jun-IRES-GFP. The murine *SCF* promoter was cloned by amplifying a 2-kb fragment from the 5′ flanking region of the *kit-ligand* (*Kitl*) gene (Table 1 lists the oligonucleotide primers), followed by its insertion into the SmaI site of the pGL3-basic luciferase reporter vector. The c-Jun wild type and c-Jun DNA$^-$ were previously described (2). For creating the AP-1 deletion mutant of the *SCF* promoter, each of the AP-1 sites (TGAC CCTCA, −1421 to −1413; TGAGTAA, −1375 to −1369; TGAATCA, −1050 to −1056; and TGAGTCA, −604 to −598) contained within the *SCF* promoter were sequentially deleted by in vitro mutagenesis. By making use of oligonucleotide primers lacking the AP-1 sites, the pGL3-*SCF* promoter plasmid was amplified using Phusion High-Fidelity DNA polymerase (Finnzymes Oy, Espoo, Finland) followed by DpnI digestion to remove original template plasmid. First, single-site deletion mutants were created, followed by deletion of the second, third, and fourth sites in subsequent rounds of amplifications and digestions.

Reagents and antibodies. The kinase inhibitor for MAP kinase (PD98059), Jun N-terminal kinase (SP600125), and phosphatidylinositol 3 (PI3)-kinase (LY294002) were obtained from Calbiochem EMD Bioscience (San Diego, CA). The p38 MAP kinase inhibitor (SB203580) was from Tocris Cookson Inc. (Ellisville, MO), epidermal growth factor (EGF) was obtained from Biosource International (Camarillo, CA), transforming growth factor β (TGF-β) was from Promega (Madison, WI), and interleukin-1 (IL-1) and tumor necrosis factor alpha were from Sigma-Aldrich (St. Louis, MO). SCF from Peprotech Inc. (Rocky Hill, NJ), anti-c-Jun antibody (H-79; Santa Cruz Biotechnology, Santa Cruz, CA), anti-GDI (RTG Sol, Gaithersburg, MD), anti-SCF antibody (R&D Systems, Minneapolis, MN), and rhodamine-anti-phalloidin and DAPI (4′,6′-diamino-2-phenylindole) (both from Sigma-Aldrich Corp., St. Louis, MO) were also used. Biodipy 650/665 anti-phalloidin was from Molecular Probes, Inc. (Eugene, OR).

Cell culture, viral cell transduction, and reporter gene assays. Cells were maintained in Dulbecco's modified Eagle's medium (DMEM) supplemented with 10% fetal bovine serum and 100 μg/ml (each) of penicillin and streptomycin and were cultured in 5% CO_2 at 37°C. Adenovirus propagation was previously described (65). Infection was done at a multiplicity of infection (MOI) of 20, cells were cultured overnight, and medium was changed prior to experimental analysis. Retroviral infections were conducted as previously described (65). Transfections were conducted using Genejuice transfection reagent (EMD Biosciences, San Diego, CA) and Lipofectamine (Invitrogen Corp, Carlsbad, CA) as described previously (7). Statistical analysis was conducted using a Mann-Whitney U test.

Microscopy and phalloidin staining for F-actin quantitation. Immunopositive MSCV-IRES-GFP- and MSCV-c-jun-IRES-GFP-transduced cells were examined in six-well plates. Phase-contrast microscopy and fluorescent imaging were carried out using the 20× and 60× objectives of an Olympus LSM-5 Meta Laser confocal scanning microscope. Rhodamine-phalloidin F-actin staining was conducted as previously described (35). F-actin quantitation was also carried out by fluorescence-activated cell sorting analysis (40). Briefly, confluent c-*jun*$^{f/f}$ cells treated with adenoviruses were harvested and washed with phosphate-buffered saline (PBS). Cell pellets were fixed with paraformaldehyde and permeabilized with Triton X-100. Following a wash with PBS, cells were stained with 0.6 μM biodipy 650/665 phalloidin (Molecular Probes, Eugene, OR) in PBS for 10 min at room temperature (64).

Cells were plated on fibronectin-coated glass coverslips and grown to approximately 80% confluence, and scanning electron microscopy was conducted as described previously (35).

Cell adhesion assay. Ninety-six-well cell surface matrix-coated strip-well tissue culture plates (no coating, collagen I, collagen IV, poly-L-lysine, laminin, fibronectin, and vitronectin) were used for cell adhesion assays. Equal numbers of cells were seeded at the bottom of each coated well and allowed to adhere by incubating the plates at 37°C in 5% CO_2 for planned intervals. Strip-wells containing adherent cells were removed at 30 min, 1 h, 1.5 h, 2 h, 3 h, and 4 h; cells were fixed in 1% glutaraldehyde for 10 min and stained with 0.1% crystal violet for 30 min. Following PBS washes, 100 μl of 0.5% Triton X-100 was added to each well to lyse the cells and extract dye by incubating the plates overnight at room temperature with gentle shaking. Quantitation of extracted dye was conducted by measuring the absorbance at 595 nm. For each cell surface matrix, the background was noted from a coated well with no cells seeded and subtracted to obtain the actual values of absorbance at 595.

Assays of cell motility, migration, and invasion. Cells were plated on plastic dishes coated with 10 μg/ml fibronectin and cultured overnight in DMEM containing 5% fetal bovine serum. Cell movements were monitored using a Zeiss inverted microscope. Video images were collected with a charge-coupled-device camera (model 2400) at planned intervals, digitized, and stored as images using Metamorph, version 3.5, software (18). Images were converted to QuickTime movies, and the positions of nuclei were tracked to quantify cell motility. Cellular velocity was calculated in micrometers using Metamorph software. The effect of kinase inhibitors on cell migration were determined after culturing the cells with 25 μM PD98059, 25 μM LY294002, 25 μM SB203580, 25 μM SP600125, 10 μM Y27632, 10 μM H-1152, and 10 μM HA-1100 (6, 10, 27, 47, 49, 67). Prior to an examination for effects on cell motility, analyses were conducted for 3 h. At this time point, the persistence for migratory directionality was determined as a relative *D*/*T* ratio representing the ratio of the direct distance (*D*) from start point to end point divided by the total track distance (*T*) (18). Net displacements were measured every 15 min from start point to end point. Data from at least 100 cells were collected for each set or treatment.

Migration of cells across a membrane was determined using a Boyden chamber, as previously described (31, 32). A gradient of SCF was created through the addition of SCF (0.5 ng/ml) to the lower chamber. Analysis of three-dimensional invasive activity was conducted as previously described (44). A total of 10^5 cells were embedded in 100 μl of collagen in a 96-well plate and cultured for 24 h. The collagen-cell plugs were transferred to 24-well plates and embedded in 1 ml of collagen and cultured for 5 days. Migration from the central plug into the surrounding collagen was monitored by phase-contrast microscopy.

Cytokine array analysis. Mouse cytokine arrays spotted on nitrocellulose membranes were obtained from Raybiotech (Norcross, GA). Conditioned medium from Ad-Null- and Ad-Cre-treated c-*jun*$^{f/f}$ cells was prepared by culturing cells in serum-free DMEM for 24 to 48 h. Membranes were then processed according to the manufacturers' instructions for assessment of secreted cytokines and growth factors present in conditioned medium.

Real-time PCR, ChIP assays, and enzyme-linked immunosorbent assay (ELISA). All gel-based PCRs and reverse transcription-PCRs (RT-PCRs) were done with an ExTaq DNA Polymerase kit (Takara Shuzo, Shiga, Japan) using the oligonucleotide primers listed in Table 1. RNA was extracted using a standard guanidinium isothiocyanate method, RQ1 DNase I (Promega, Madison, WI) treated, and phenol-chloroform extracted. RNA quantitation was done in an Agilent 2100 Bioanalyzer (Palo Alto, CA), and equal quantities were used for the reverse transcription reactions. Primers for all the genes including housekeeping control gene transcripts were either designed using Primer Express 5.1 (Applied Biosystems Inc., Foster City, CA) (Table 1) or referenced from Sugimoto et al. (54). Chromatin immunoprecipitation (ChIP) analysis was performed according to a standard protocol provided by Upstate Biotechnology, Inc., with minor modifications (14, 22). PCR amplifications were done using a Takara ExTaq Kit and oligonucleotide primers listed in Table 1. PCR amplification was carried out for a region not containing any AP-1 site within the SCF promoter to serve as a control (negative) for sonication.

For ELISA, cells were seeded at 80% of confluence, and the growth medium was changed 24 h later to basal medium containing 0.1% bovine serum albumin after samples were washed with PBS. Forty-eight hours later, the conditioned medium was collected, and supernatant was obtained by centrifugation at 2,000 rpm for 5 min, followed by filtration through a 0.45-μm-pore-size membrane filter. SCF in the conditioned medium was measured using a mouse SCF ELISA kit (Raybiotech, Narcross, GA) in triplicate, as per the manufacturer's recommendations, and normalized by the total protein levels in the medium of each individual sample. The TGF-β and EGF ELISA assays were conducted using a mouse TGF-β Quantikine ELISA Kit (R&D Systems, Inc., Minneapolis, MN) (11) and a Mouse EGF Quantikine ELISA kit (R&D Systems, Inc., Minneapolis, MN) (8), respectively. Experiments were conducted at least three separate times.

Measurement of ROCK activation. Rho-associated protein kinase (ROCK) activation was assessed by a CycLex Rho kinase assay kit (Cyclex Co., Ltd., Nagano, Japan) which uses the myosin-binding subunit of myosin phosphatase as a substrate (59). To exclude the activity of other kinases from the results, the absorbance values obtained from ROCK inhibitor-treated lysates were subtracted from total absorbance.

RESULTS

Endogenous c-Jun inhibits cellular adhesion. In order to examine the role of c-Jun in guided migration, conditional knockout mice in which the c-*jun* gene is flanked by *loxP* sites were used. MEFs derived from these mice (c-*jun*$^{f/f}$) were cultured (60) and transduced with either adenovirus-expressing Cre or an equal titer of adenovirus-null virus. Analyses were conducted within 48 h of transduction with Ad-Cre. PCR and RT-PCR confirmed the deletion of c-*jun* in DNA and the presence of expressed Cre mRNA transcripts in cellular RNA. Equal amounts of amplification of RPL-19 in DNA and RPL-19 transcripts in RNA served as housekeeping gene controls for the PCR and RT-PCR amplification reactions (Fig. 1A and B). Expression of Cre recombinase resulted in deletion of c-Jun and loss of c-Jun protein by Western blot analysis when normalized to the protein loading control GDI (Fig. 1C). No inhibitory effect of either the Ad-Cre or Ad-null virus on proliferation of cells was observed, consistent with recent studies (45). To determine whether c-Jun regulates cellular diameter in suspension, the diameters of cells were assessed using a Multisizer Z3 (Beckman Coulter Inc, Miami, FL). Cell diameters in suspension were identical for the c-*jun*$^{+/+}$ and c-*jun*$^{-/-}$ cells (Fig. 1D), but c-*jun*$^{-/-}$ cells adhered to tissue culture plates showed greater cellular spreading by phase-contrast microscopy (Fig. 1E); this observation warrants further analysis.

To examine the morphology of cells deleted of c-Jun, scanning electron microscopy was conducted (Fig. 2A). Fibroblasts demonstrated an elongated bipolar fibroblastoid shape, either in the absence of adenovirus or in the presence of a control adenovirus. The addition of adenovirus-expressing Cre resulted in both c-*jun* excision and a change in cellular morphology. Cells deleted of c-*jun* were rounder and flatter (Fig. 2A). Stress fiber formation assessed by phalloidin (Fig. 2B) confirmed the spread morphology and demonstrated a peripheral distribution of stress fibers in c-*jun*$^{-/-}$ cells (Fig. 2B). In order to examine whether the round morphology of c-*jun*$^{-/-}$ cells correlated with increased cellular adhesion, assays were conducted on distinct substrata (Fig. 2C). Adhesion analyses were conducted at several time points. In order to determine the effect of substratum adhesion, a comparison was made between c-*jun*$^{-/-}$ and c-*jun*$^{+/+}$ cells at 30 and 240 min. c-*jun*$^{-/-}$ cells were more adherent than c-*jun*$^{+/+}$ cells at 240 min. For ease of comparison of the effect of the substratum upon the increase in adhesion, at initial contact (30 min) was normalized to 100%. A relative increase in adhesion was observed in c-*jun*$^{+/+}$ versus c-*jun*$^{-/-}$ for cells plated on laminin and vitronectin (Fig. 2C and D).

c-Jun enhances cellular migratory velocity. The speed of wound closure represents the combination of several factors including migratory velocity and persistence of migratory di-

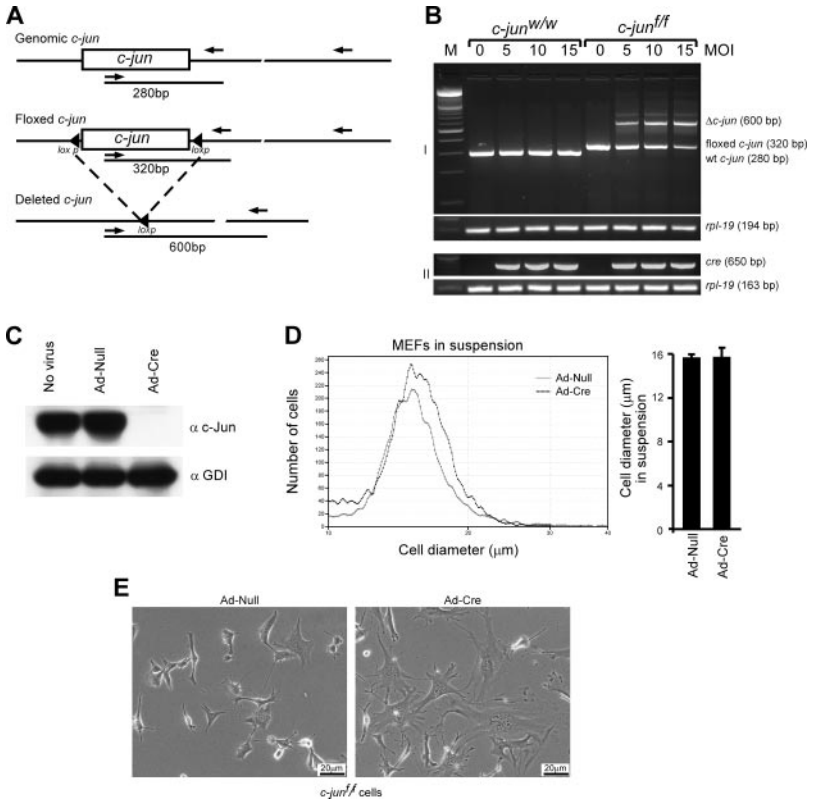

FIG. 1. Somatic excision of c-*jun* in mouse embryo fibroblasts induces a spread cellular morphology. (A) Schematic outline of the genomic wild-type (c-*jun*), floxed (c-$jun^{f/f}$), and deleted c-*jun* (c-jun^{Δ}) locus with *loxP* sites (◀) and PCR primer binding sites (→). (B) PCR showing excision of c-$jun^{f/f}$ alleles (I). Lanes 1 to 4, wild-type c-$jun^{+/+}$; lanes 5 to 8, c-$jun^{f/f}$ DNA. All sample lanes were treated with Ad-Cre at various MOIs of virus as indicated. RT-PCR from the RNA shows expression of Cre in Ad-Cre treated fibroblast cells (II). (C) Western analysis of (c-$jun^{f/f}$) cells with no virus, Ad-Null-, and Ad-Cre-treated (MOI of 20) cells analyzed for the presence of c-Jun protein in the lysates; GDI was used as loading control. (D) Cell diameter measurements (in suspension) of Ad-Null- and Ad-Cre-treated c-$jun^{f/f}$ cells determined on cells in suspension. (E) Spread morphology of Ad-Null- and Ad-Cre-treated c-$jun^{f/f}$ cells growing in culture adhering to the tissue culture plate.

rectionality (18). Video microscopy was undertaken of wound closure (Fig. 3A and B) to determine a detailed analysis of the cellular velocity of c-Jun-deficient cells (Fig. 3C). Wound closure was delayed in c-$jun^{-/-}$ cells (Fig. 3B). The c-$jun^{-/-}$ cells showed reduced (~45%) cellular velocity (Fig. 3C) ($P < 0.05$).

The relatively greater defect in wound closure rate compared with the reduction in cellular velocity of c-$jun^{-/-}$ cells suggested that a defect in directional persistence may contribute to defective wound closure. Analysis was therefore conducted of the persistence of migratory directionality (PMD). Representative examples of cell movement plated on fibronectin-coated slides tracked at 15-min intervals over 3 h were used to determine the role for c-Jun in persistence of migratory directionality (Fig. 3D). The quantitation of PMD was undertaken using a relative D/T ratio, representing the ratio of direct distance from the start point to the endpoint divided by the total track distance (18). c-Jun-deficient cells showed a 66% reduction in persistence of directionality (Fig. 3D).

To determine whether c-Jun was sufficient to reverse the defect in cellular migration, c-$jun^{-/-}$ MEFs were transduced with a retroviral expression vector encoding c-Jun. c-$jun^{f/f}$ cells were transduced with Ad-Cre or Ad-control and then sequentially transduced with a retrovirus expression vector encoding IRES-GFP or c-Jun-IRES-GFP. Reanalysis was conducted 48 h posttransduction with the retrovirus encoding c-Jun. c-Jun expression reversed the defect in cellular velocity and migratory directionality (Fig. 4).

The effect of c-Jun on the cellular area of adherent cells was next assessed. Deletion of c-*jun* increased the cellular area (Fig. 5A and C). Reintroduction of c-*jun* by viral transduction, reduced the cellular area compared to that of wild-type control cells (Fig. 5A and C). Studies were undertaken to determine whether c-Jun was capable of rescuing the defect in cellular migration, or whether the defect in migration was being maintained by secondary effects, independent of c-Jun. Reintroduction of c-*jun* into the c-$jun^{-/-}$ cells also rescued the abundance of c-Jun protein, which was very similar to c-$jun^{+/+}$ cells, as assessed by Western blot analysis (Fig. 5B). Compared with c-$jun^{+/+}$ cells, c-$jun^{-/-}$ cells displayed a threefold increase in cellular area. Reintroduction of c-Jun into c-$jun^{-/-}$ cells restored the cellular area to that of c-$jun^{+/+}$ cells (Fig. 5C).

SCF is secreted in response to endogenous c-Jun and promotes cellular migration. Earlier coculture experiments of human keratinocytes and c-$jun^{-/-}$ fibroblasts identified IL-1 as a c-Jun target gene regulating keratinocyte differentiation through paracrine secretion (56). To consider the possibility that c-Jun may regulate the secretion of paracrine factors, which in turn contribute to fibroblast migration, conditioned

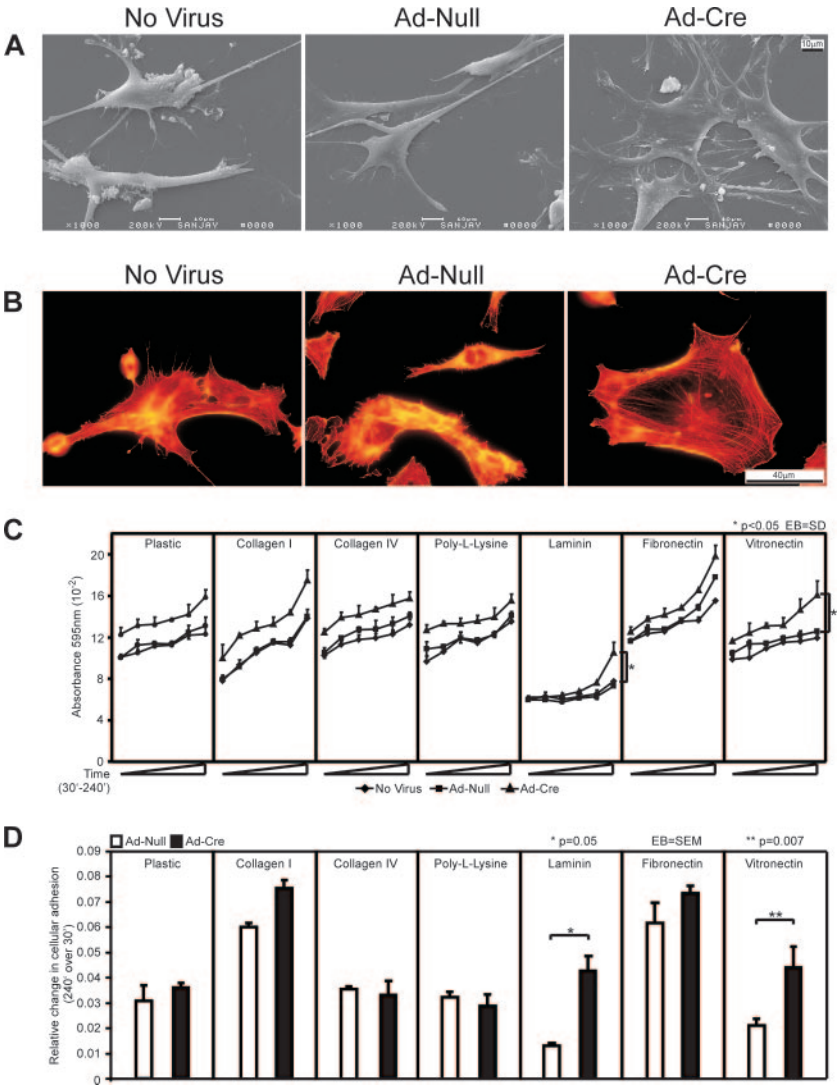

FIG. 2. c-Jun regulates cellular spreading and adhesion. (A) Scanning electron micrographs of c-*jun*$^{f/f}$ cells treated with either no virus, Ad-Null, or Ad-Cre. Note the Ad-Cre-treated c-*jun*$^{f/f}$ cells show a flattened appearance after c-*jun* excision. (B) Rhodamine-phalloidin staining for F-actin of untreated, Ad-Null, and Ad-Cre-treated c-*jun*$^{f/f}$ cells. Peripheral staining of F-actin is observed in Ad-Cre-treated cells (deleted of c-*jun*). Note that c-*jun*$^{-/-}$ cells show greater spreading in comparison to c-*jun*$^{+/+}$ cells (untreated or Ad-Null-treated cells). Magnification, ×600 (60× objective and 10× eyepiece). (C) Cellular adhesion assay comparing c-*jun*$^{f/f}$ MEFs treated with either Ad-Null or Ad-Cre. Cells were plated on distinct substrata as indicated and analysis was conducted at six time points (30 min to 240 min). The data are shown as mean ± standard deviations of three separate experiments. (D) The substratum-induced adhesion is shown as difference in adhesion at 4 h and 30 min in Ad-Cre- versus Ad-Null-treated c-*jun*$^{f/f}$ cells.

medium from c-*jun*$^{+/+}$ cells was added to the c-*jun*$^{-/-}$ cells. The conditioned medium of c-*jun*$^{+/+}$ cells rescued the migratory characteristics of c-*jun*$^{-/-}$ cells including cellular migration velocity and PMD (Fig. 6A). The medium from c-*jun*$^{+/+}$ cells restored the defective PMD of c-*jun*$^{-/-}$ cells, indicating a key role for secreted factors in defective migration of c-*jun*$^{-/-}$ cells (Fig. 6). Neither IL-1 nor tumor necrosis factor alpha rescued the PMD defect of c-*jun*$^{-/-}$ cells (data not shown).

In view of the ability of conditioned medium from c-*jun*$^{+/+}$ cells to rescue the defective migration of c-*jun*$^{-/-}$ cells, an unbiased proteomic analysis was conducted to screen for additional candidate cytokines and growth factors contributing to cellular migration. A cytokine and growth factor array approach was used, conducting subtractive comparison of medium from c-*jun*$^{+/+}$ and c-*jun*$^{-/-}$ cells. Multiplicative quantitative studies demonstrated that the abundance of most proteins was unaltered by c-Jun deletion (Fig. 7A; see Fig. S1 in the supplemental material). The abundance of SCF was, however, reduced by 35% (Fig. 7A). In order to determine the mechanisms by which c-Jun regulated SCF abundance, an ELISA was conducted for secreted SCF in conditioned medium (Fig. 7B). c-*jun* deletion reduced SCF protein abundance from 500 pg/ml to 200 pg/ml (Fig. 7B). The mRNA levels of the secreted (*KL-1*) and membrane-bound (*KL-2*) forms of SCF were determined by real-time quantitative RT-PCR from c-*jun*$^{f/f}$ cells treated with Ad-Null and Ad-Cre (Fig. 7C). The relative quantitation data obtained from real-time quantitative RT-PCR shown in the Fig. 7C was normalized to expression of

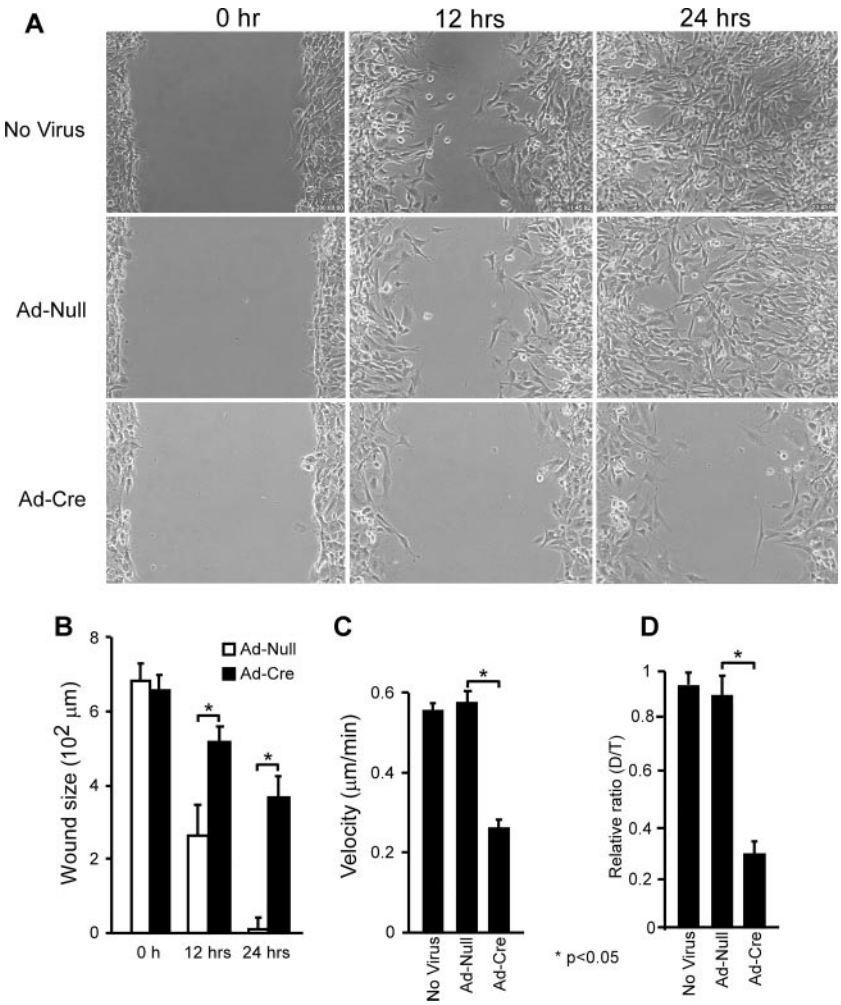

FIG. 3. c-*jun* excision reduces cellular migration rates. Wound healing assay of untreated, Ad-Null-, or Ad-Cre-treated c-$jun^{f/f}$ cells. (A) Cells were imaged every 15 min by video microscope for 24 h. Representative images at 0, 12, and 24 h are shown. c-$jun^{-/-}$ cells showed reduced wound closure at 24 h. Graphs show wound size (B), migration velocity (C), and PMD (D) at 0, 12, and 24 h. *D*/*T* calculations were based on data collected after analysis of video images for cell movement every 15 min for 3 h. Data are shown as means ± standard error of the means for more than three separate experiments. *, $P < 0.05$.

the housekeeping gene 18S rRNA using ABI SDS 2.1 software. SCF mRNA levels were reduced more than 80% in c-$jun^{-/-}$ cells compared with the wild-type control (Fig. 7C). Several other known c-Jun target genes assessed as a form of positive control also showed reduced expression in c-$jun^{-/-}$ cells, including *twist homolog 1*, *twist homolog 2*, and *twist neighbor* (Fig. 7D).

To determine whether the reduction in SCF abundance in c-$jun^{-/-}$ cells contributed to the defect in cellular migration, c-$jun^{-/-}$ cells were treated with SCF. The addition of 0.5 ng/ml SCF completely reversed the defect in cellular migration (Fig. 8A) velocity and directionality (Fig. 8 B and C, bars 7 versus 8). Immunoneutralizing antibody to SCF was used to examine its ability to inhibit migration of c-$jun^{+/+}$ cells. SCF immunoneutralization reduced cellular velocity and persistence of migratory directionality by 40% (Fig. 8B and C, bars 4 versus 6). Collectively, these studies suggest that the reduced SCF production in c-$jun^{-/-}$ contributes to the defect in velocity and directionality of cellular migration. To determine whether the increased cellular adhesion observed in c-$jun^{-/-}$ cells (Fig. 2) was a function of defective SCF secretion, adhesion assays were conducted. Addition of SCF reduced cellular adhesion of c-$jun^{-/-}$ cells particularly when cells were plated on laminin or vitronectin (Fig. 8D).

Transmigration or migration across a cellular membrane was next assessed using a Boyden chamber. c-$jun^{-/-}$ cells were defective in transmigration compared with c-$jun^{+/+}$ cells (Fig. 9A). The addition of SCF (0.5 ng/ml) promoted transmigration of c-$jun^{-/-}$ cells and fully rescued the defect in transmigration, while immunoneutralizing antibody to SCF reduced migration of c-$jun^{+/+}$ cells by 40% (Fig. 9B). The restoration of c-$jun^{-/-}$ cellular transmigration by SCF is consistent with a role of reduced SCF production leading to a migration defect. In order to determine the role of c-*jun* in cellular invasion, the ability of cells to invade a collagen matrix in three dimensions was assessed (44). The invasive phenotype displayed by cells negotiating three-dimensional extracellular matrix barriers is a more complex form of cellular behavior and may more closely

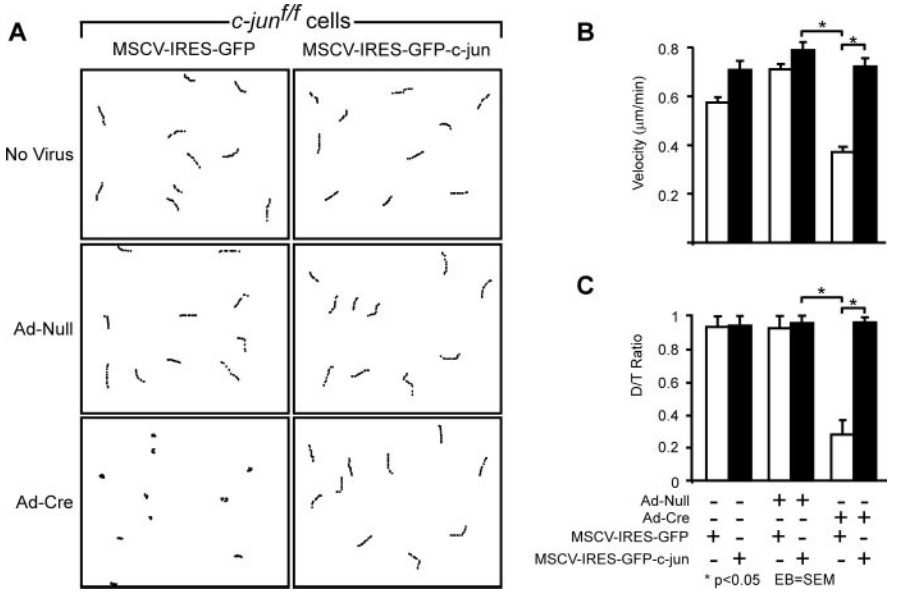

FIG. 4. c-Jun rescues the migration defect of c- *jun*$^{-/-}$ cells. c-*jun*$^{f/f}$ cells transduced with Ad-Cre to excise c-*jun*$^{f/f}$ 48 h postexcision were retransduced with retrovirus expressing either GFP or c-Jun. Video microscopy demonstrated induction of migration by c-Jun expression and rescue of cellular migration in c-*jun*$^{-/-}$ cells. (A) Path tracings of cellular movements. (B) Quantitation of cellular velocity. (C) Persistence of directionality of migration. EB, error bar; SEM, standard error of the mean.

resemble the in vivo function of c-Jun. Invasion of collagen was assessed by the detection of refractile cells distal to the cellular margin after 5 days. Deletion of c-*jun* virtually abolished the ability of cells to invade the collagen in a three-dimensional matrix (Fig. 10B). Addition of SCF (0.5 ng/ml) rescued the invasive phenotype of c-*jun*-deficient cells. Immunoneutralizing antibody to SCF reduced the number of cells invading collagen by 23% (Fig. 10E versus F).

SCF is a direct target gene induced by c-Jun. To determine whether the *SCF* gene was a direct transcriptional target of c-Jun, a 2.0-kb fragment of the murine *SCF* promoter was cloned and linked to a luciferase reporter gene. Sequencing of

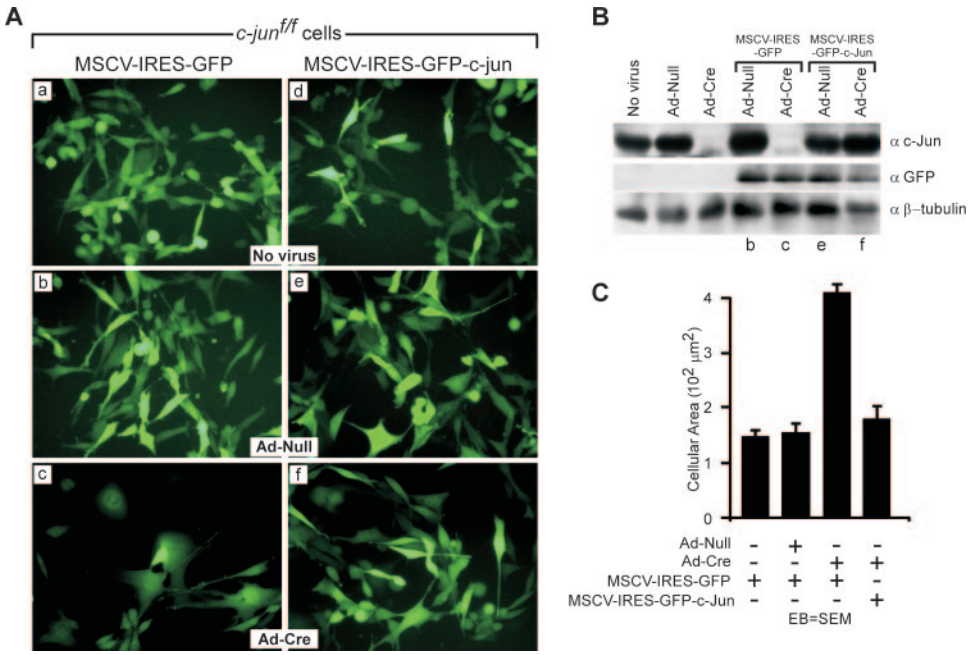

FIG. 5. c-*jun* rescues cellular morphology of c-*jun*$^{-/-}$ cells. IRES-GFP- or c-Jun-IRES-GFP-expressing MSCV vectors were transfected into untreated, Ad-Null-, or Ad-Cre-treated c-*jun*$^{f/f}$ cells. (A) Fluorescence microscopy of c-*jun*$^{-/-}$ (c) versus cells rescued with c-*jun* (f). (B) Western blot analysis of the MEFs either deleted of c-*jun* or rescued with c-*jun*. GFP is expressed by the MSCV vectors used. (C) Cellular area determined using NIH Image software. EB, error bar; SEM, standard error of the mean.

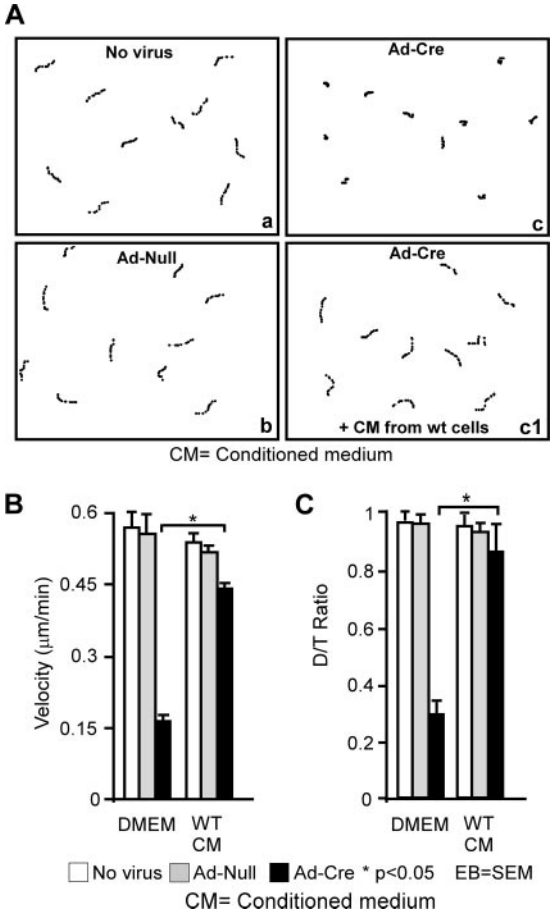

FIG. 6. Conditioned medium from c-*jun*$^{+/+}$ cells rescues the defective migratory response of c-*jun*$^{-/-}$ cells. (A) Path tracings from PMD assays conducted on untreated (a), Ad-Null (b), Ad-Cre (c), and Ad-Cre c-*jun*$^{f/f}$ cells treated with conditioned medium (d) from c-*jun*$^{+/+}$ cells. Treatment of Ad-Cre-infected cells with conditioned tissue culture medium (CM) from wild-type cells rescued their defective cellular migration (cellular velocity) (B) and persistence of direction (C) (*D*/*T* ratio). EB, error bar; SEM, standard error of the mean.

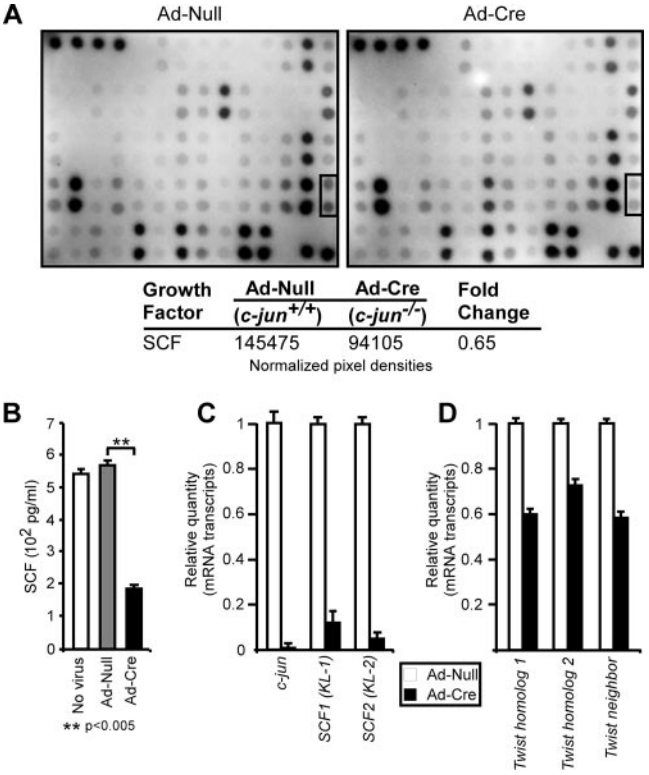

FIG. 7. c-*jun* induces SCF secretion and expression. (A) The supernatant of c-*jun*$^{+/+}$ and c-*jun*$^{-/-}$ cells was analyzed by cytokine and growth factor arrays. Supernatant from c-*jun*$^{+/+}$ cells that rescued a c-*jun*$^{-/-}$ cellular migration defect was assessed. Representative data of three separate experiments are shown. Mean data of the SCF abundance are shown (see Fig. S1 in the supplemental material for names of the proteins assayed in the array). (B) ELISA for SCF abundance in conditioned medium from c-*jun*$^{f/f}$ cells treated with no virus, Ad-Null, and Ad-Cre. (C) Real-time RT-PCR quantification of c-*jun*, SCF (*KL-1*, soluble form; *KL-2*, membrane-bound form) transcripts of *KL* gene for SCF. (D) Real-time RT-PCR quantitation of known c-*jun* target genes (*twist 1*, *twist 2*, and *twist neighbor*). In all real-time quantitative RT-PCR assays, the data for the gene of interest were normalized to the expression of transcripts for the 18S rRNA housekeeping control gene.

the *SCF* promoter demonstrated the presence of a canonical AP-1 binding site(s) (Fig. 11). The activity of the murine *SCF* promoter was reduced by 80% in c-*jun*$^{-/-}$ cells when normalized for transfection efficiency using the *Renilla* luciferase reporter gene, pRL-LUC (Fig. 11A). Transfection of c-*jun*$^{-/-}$cells with an expression vector for c-Jun induced SCF-Luc reporter activity sixfold compared with the effect of expression of a DNA-binding-defective mutant of c-Jun (c-Jun DNA^{-}) (Fig. 11B). In order to determine whether the *SCF* promoter functioned as direct transcriptional target, deletion mutation of the *SCF* promoter AP-1 sites was conducted. Comparison was made between the *SCF-wt* and *SCF-AP-1* mutant promoters. c-Jun induced the *SCF* promoter but failed to induce the *SCF-AP-1* mutant promoter (Fig. 11C). The *SCF* promoter was 5- to 10-fold more active than the luciferase vector control in the presence of c-*jun* while the *SCF-AP-1* mutant reporter conveyed basal activity to the luciferase vector under identical conditions. The finding suggests that the AP-1 sites function as both basal level and c-Jun-responsive enhancer elements.

To determine whether c-Jun bound the *SCF* promoter in the context of local chromatin, ChIP assays were conducted. Oligonucleotide primers designed to the proximal *SCF* promoter (designated "negative" in Fig. 11D) failed to amplify genomic *SCF* sequence in the presence of the c-Jun immunoprecipitate, indicating the efficiency of sonication. Amplification of *SCF* promoter sequences was observed with primers directed to the AP-1 site and three other AP-1 like elements in the *SCF* promoter. ChIP assays conducted on c-*jun*$^{f/f}$ cells treated with Ad-Cre abrogated c-Jun occupancy at the *SCF* promoter AP-1 site (Fig. 11D). Thus, c-Jun induces SCF protein and mRNA abundance and c-Jun induces the *SCF* promoter through a DNA-binding-dependent mechanism.

DISCUSSION

The current studies demonstrate an essential role for c-Jun in regulating the velocity of cellular migration and directional persistence. Wound healing is known to induce the expression of AP-1 transcription factors (16). c-Jun together with Jun-B,

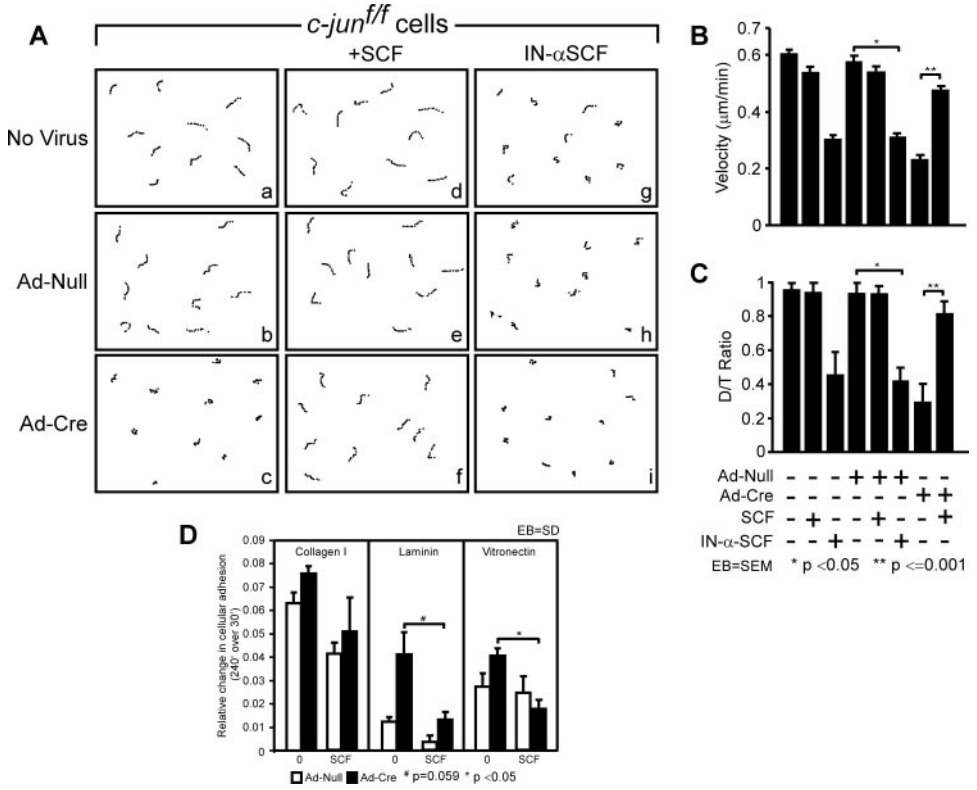

FIG. 8. SCF rescues migration defect of c-*jun*$^{-/-}$ cells. (A) Path tracings for c-*jun*$^{f/f}$ cells treated with Ad-Cre and either an immunoneutralizing antibody to SCF (IN-αSCF) (1 μg/ml) or the addition of SCF (0.5 ng/ml). Data for more than three experiments are shown. Data for quantitation of cell migration parameters, including velocity of migration (B) and the D/T ratio to assess persistence of migratory directionality (C) are shown. (D) Cellular adhesion assays were conducted as described in the legend of Fig. 2, with the addition of SCF (0.5 ng/ml) on various matrices (collagen I, laminin, and vitronectin). Substratum adhesion is shown as the difference between 4 h and 30 min. EB, error bar; SEM, standard error of the mean.

c-Fos, and FosB is induced within 1 h of wounding of corneal epithelium (50). It has been proposed that AP-1-dependent activation of a subset of genes including keratins and integrins, in turn, contributes to the epithelial cell migration response to wounding (4, 5). The AP-1 transcription factors induce production of matrix metalloproteases and plasminogen activator, providing a mechanism by which cells move into the extracellular matrix. Herein, video microscopy demonstrated a reduction in the migratory velocity of cells acutely deleted of c-*jun*. The defect in migratory persistence of c-*jun*$^{-/-}$ cells was res-

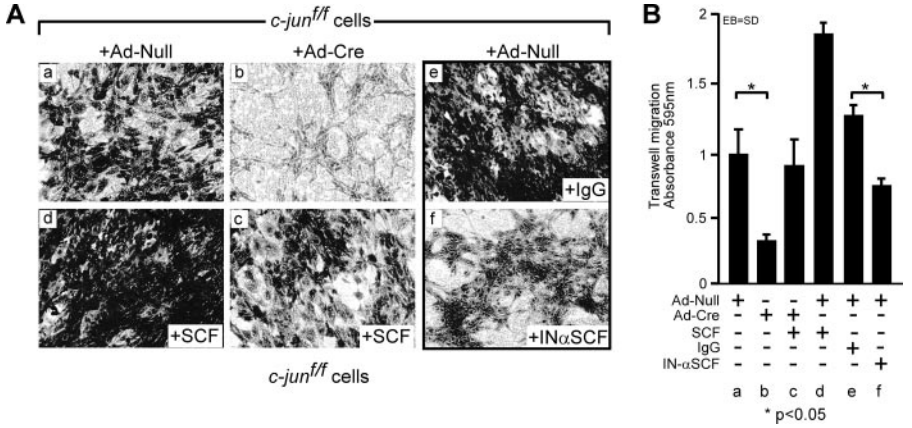

FIG. 9. SCF rescues the transwell cellular migration defect of c-*jun*$^{-/-}$ cells. c-*jun*$^{f/f}$ cells were treated with Ad-Cre and analyzed for transwell migration. Cells traversing the membrane were stained blue with crystal violet and appear lighter in the images. The effect of immunoneutralizing antibody to SCF or addition of SCF (0.5 ng/ml) on transwell migration was quantitated for more than five separate experiments. (B) Data are shown as the means ± standard deviations (SD). *, $P < 0.05$. IgG, immunoglobulin G; IN-αSCF, immunoneutralizing antibody to SCF; EB, error bar.

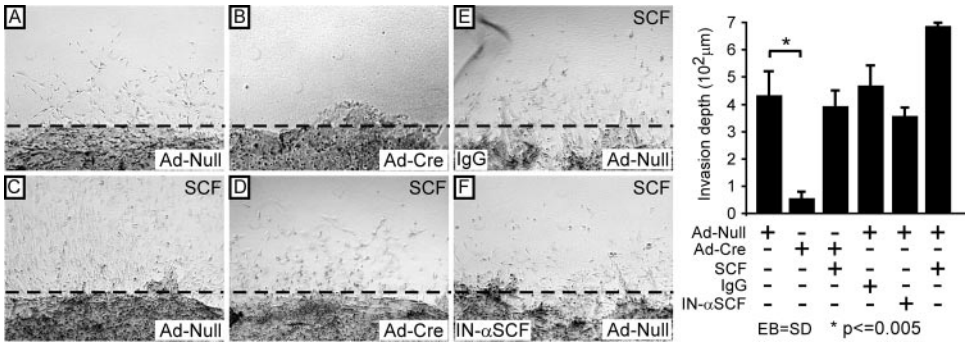

FIG. 10. SCF rescues three-dimensional collagen invasion defect of c-*jun*$^{-/-}$ cells. c-*jun*$^{f/f}$ cells were treated with Ad-Null or Ad-Cre and analyzed for invasion within three-dimensional collagen gels with or without SCF (0.5 ng/ml), immunoglobulin G (IgG), or immunoneutralizing antibody against SCF (IN-αSCF). The edge of the embedded island of fibroblasts is marked by a dashed line on each panel. Invasion was quantitated in three-dimensional collagen gels after 5 days in the presence of SCF or following the addition of immunoneutralizing antibodies against SCF. EB, error bar; SD, standard deviation.

cued through supernatant derived from fibroblasts expressing c-Jun or with the addition of SCF, consistent with a role for c-Jun in regulating autocrine secretion of factors that promote cellular migration. c-*jun* deletion reduced SCF protein abundance, mRNA, and promoter activity. c-Jun expression induced the *SCF* promoter and bound the *SCF* promoter's AP-1 sites in ChIP assays. These findings define a new role for c-*jun* in regulating SCF expression and, thereby, cellular invasion.

SCF induced migration of c-*jun*$^{-/-}$ cells, suggesting that the receptor, Kit, maintains normal function in the absence of c-Jun and confirming the biological importance of SCF as a c-Jun target gene. In addition to serving as a growth factor for various cell types, including hematopoietic stem cells, mast cells, melanocytes, and germ cells, SCF has chemotactic properties for endothelial cells, functioning as a proangiogenic factor (55). Complete absence of SCF, which is encoded by the mouse steel locus (S1), or Kit kinase, leads to embryonic or perinatal lethality from anemia. In humans, gain-of-function mutations of c-*kit* occur in human cancers (gastrointestinal stromal tumors, mystocytomas, T-cell lymphomas, and dysgerminomas [19]), and paracrine or autocrine activation of *kit* has been implicated in other human malignancies including ovarian and lung cancers (25). The correlation between Kit expression and functional measurements of pluripotentiality suggests that *kit* may be a useful marker for stem cells (38). SCF expression is upregulated in tumors in a grade-dependent manner, and high SCF expression correlates with short patient survival (55). Tumor cells with the strongest SCF expression are found within the tumor-infiltrating border, and c-*jun* is expressed predominantly at the infiltrating tumor edge (63). Collectively, these studies are consistent with a model in which c-Jun-mediated SCF production may contribute to tumor progression.

Both TGF-β and EGF have been implicated in cellular migration during *Drosophila* development (72). Neither TGF-β or EGF were represented on the arrays used. TGF-β and EGF production was reduced in c-*jun*$^{-/-}$ MEFs, as determined by ELISA, approximately 25% and 60%, respectively (see Fig. S1B in the supplemental material). We examined the possibility that TGF-β or EGF may also promote migration of c-*jun*$^{-/-}$ cells. Although addition of supraphysiological concentrations of EGF (10 ng/ml) and TGF-β (10 ng/ml) rescued in part the PMD defect of c-*jun*$^{-/-}$ cells, physiological concentrations (EGF at 20 pg/ml and TGF-β at 100 pg/ml) did not rescue the migration defect (see Fig. S1C to E in the supplemental material). These findings indicate that in cells acutely deleted of c-*jun*, the receptor signaling pathway for TGF-β and EGF remains intact. Furthermore, these studies suggest that supraphysiological or pathological but not physiological concentrations of EGF and TGF-β may play a role in c-*jun*-mediated migration. TGF-β is a known target of c-Jun in mammalian cells (62). The current findings are consistent with previous studies in *Drosophila melanogaster*, in which a key role for c-*jun* kinase in cellular migration is evidenced by dorsal closure. Mutations of *hemipterous* and *basket*, the *Drosophila* homologs of human JNKK and JNK, respectively, are associated with failed closure of the dorsal cuticle. *Drosophila* JNK is activated transiently immediately prior to dorsal closure, facilitating amnio serosa contraction in adhesion complexes in adjacent cells (37). It has been proposed this activity may contribute to the anterior movement of dorsal epithelium. *Drosophila* JNK activity persists in leading-edge epithelial cells to promote ongoing expression of the TGF-β homolog *decapentaplegia* (52). *decapentaplegia* is known to promote cellular migration in an autocrine fashion at the epithelial cell edge (17). The findings herein that the c-*jun*$^{-/-}$ cellular migratory defect is rescued by supraphysiological concentrations of TGF-β suggests that the loss of TGF-β production in c-*jun*$^{-/-}$ cells may contribute to defective migration in murine fibroblasts under a subset of circumstances.

Mouse embryonic eyelid closure requires both the proliferation of epithelial cells and the migration of epithelial sheets (51, 57). Defective eyelid closure has been demonstrated in mice defective in genes encoding growth factors and their receptors, including EGF receptor (EGFR), TGF-α, activinβB, and MEKK1. The ablation of genes encoding activinβB, the TGF-β family, and ROCK I/II results in defective eyelid closure (58, 61). Thus, both the TGF-β activin, MEKK1, and JNK pathway and the TGF-α/EGFα and ERK pathway contribute to active stress fiber formation and cellular migration. The destruction of either pathway in vivo appears to result in the failure of eyelid closure in mice. As the rescue of PMD in

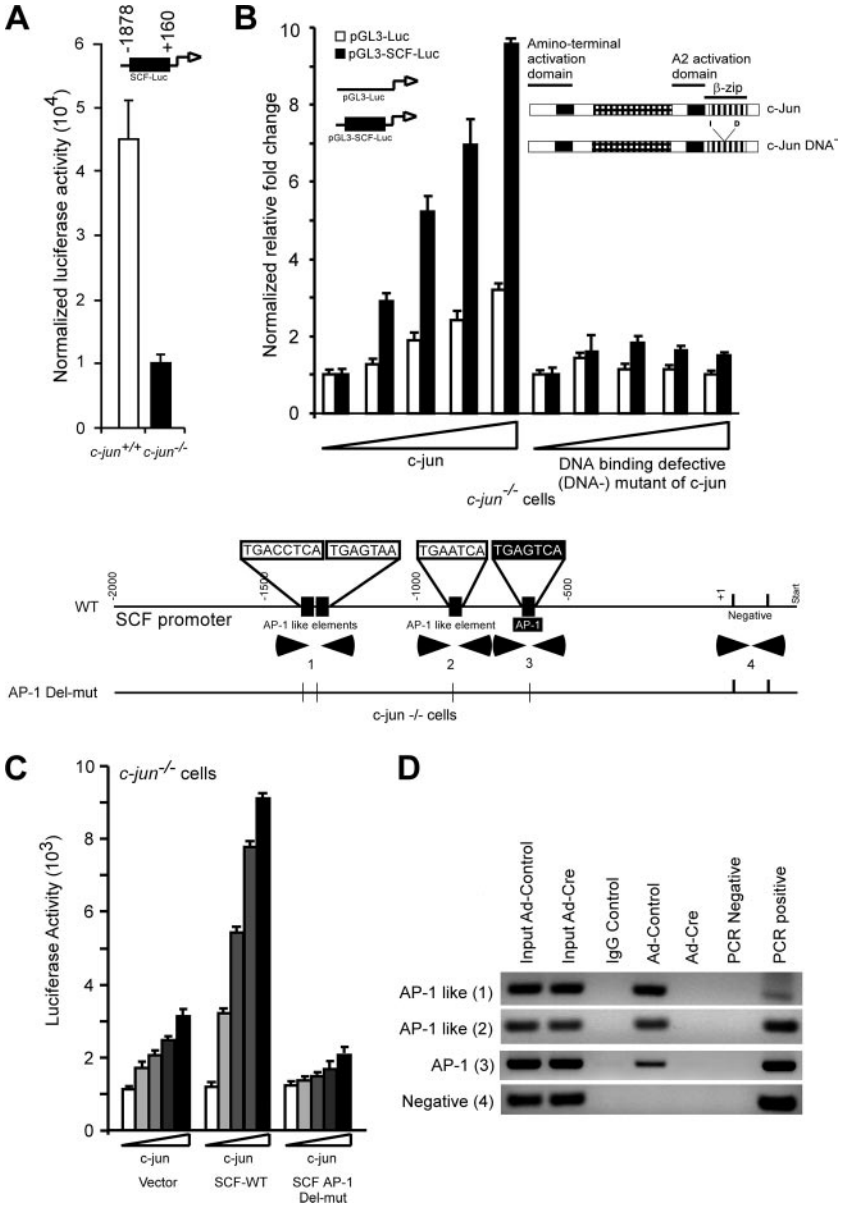

FIG. 11. c-*jun* induces SCF expression and binds to SCF promoter in ChIP assays. Schematic representation of murine *SCF* gene promoter linked to luciferase reporter gene and luciferase assay for cloned *SCF* promoter in c-$jun^{+/+}$ and c-$jun^{-/-}$ cells, effect of expression vectors coding wild-type c-Jun or DNA-binding-defective c-Jun mutant. As shown in panel A, the activity of the *SCF* promoter was assessed in c-$jun^{+/+}$ or c-$jun^{-/-}$ cells, and the luciferase activity was normalized for transfection efficiency through cotransfection with the *Renilla* luciferase reporter (psv-*Renilla*-LUC). (B) Activity of the *SCF* promoter was determined in the presence of cotransfected expression vector for either wild-type c-Jun or the DNA-binding-defective c-Jun mutant. Luciferase reporter activity is shown of transfections conducted in c-$jun^{-/-}$ cells. Data are means ± standard error of the mean of more than five separate transfections. (C) The *SCF* promoter AP-1 elements were mutated in the context of the full-length promoter. Activities of the *SCF* wild-type (WT) and *SCF*-AP-1 mutant promoters were compared in the presence of cotransfected the c-Jun expression vector. (D) ChIP assay showing recruitment of c-*jun* to the AP-1 sites in the *SCF* promoter. (E) Schematic representation of mechanism by which c-*jun* induction of SCF promotes guided migration.

c-$jun^{-/-}$ cells with EGF and TGF-β occurred acutely, the receptors and corresponding signaling pathway of these cells remained functional.

Our results contrast with studies of more prolonged c-*jun* excision in keratinocytes of these mice. K14-Cre; K5-Cre-2; c-$jun^{\Delta EP}$ mice resulted in a failure of eyelid fusion during embryogenesis, and mice were born with the "eyes open" phenotype (30, 71). c-*jun*-deficient keratinocytes expressed less phosphorylated EGFR (71), suggesting that a reduction in EGFR function may have contributed to defective migration. These differences may either relate to a cell-type-specific function of c-*jun* or reflect acute (this study) versus chronic (30, 71) effects of c-Jun deletion. Acute deletion of the retinoblastoma (*Rb*) gene in primary quiescent cells is sufficient for cell cycle reentry and has a phenotypic consequence that is different from germ line Rb functional inactivation (45). Such differ-

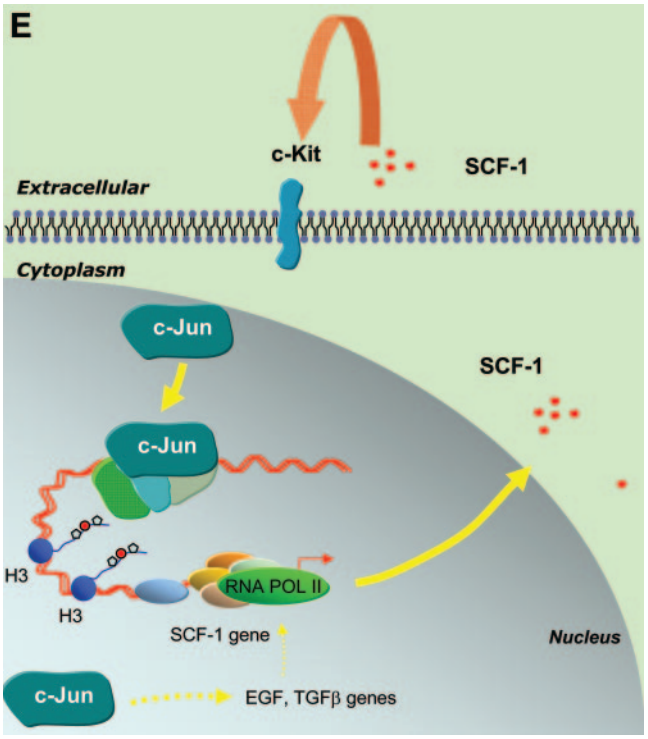

FIG. 11—*Continued.*

ences may be due to functional compensation by Rb-related proteins. Somatic excision of c-*jun* in the central nervous system blocks perineuronal sprouting, lymphocyte recruitment, and microglial activation. c-*jun*-deficient motor neurons show reduced target muscle reinervation (41). c-*jun*-deficient neurons expressed reduced galanin, α7β1, and CD44, the expression of which contributes to normal neuronal regeneration (41). It will be of interest to assess further the paracrine secretory deficiencies of c-*jun*$^{-/-}$ keratinocytes to better understand the cell-type-specific function of c-*jun* in cellular migration.

Kit activation induces multiple downstream signaling pathways including JNK, ERK, Akt, and PI3-kinase. In the current studies multiple intracellular kinase signaling pathways contributed to the migration of wild-type MEFs including the PI3-kinase, ERK, JNK, and MAP kinase pathways (see Fig. S2 in the supplemental material), consistent with previous studies implicating these kinases in fibroblast migration (20, 21). The PI3-kinase pathway has been implicated in the cellular migratory response to growth factor signals including EGF (46, 48). MAP kinase activity is known to accelerate the immediate cell motility in some, but not all, cells (9, 24). The role of candidate intracellular signaling pathways was determined. Specific inhibitors for each of the MAP kinase pathways and PI3-kinase activity were used at the dose shown in many prior studies to inhibit the relevant pathway (6) without directly affecting viability (cellular viability was confirmed in the current studies in the presence of inhibitor). The Jun kinase inhibitor SP600125 reduced basal PMD of the cells (see Fig. S2A and C in the supplemental material). This concentration of SP600125 is consistent with the dose used in previous studies (6) and did not affect cell viability. The PI3-kinase inhibitor LY 294002 did not affect PMD but blocked Ras activation of a multimeric AP-1 reporter gene in our previous studies (3). Both the p38 and ERK inhibitors (SB203580 and PD98059) reduced basal level PMD. The ROCK inhibitor Y27632 did not affect wild-type MEF migration but enhanced c-*jun*$^{-/-}$ MEF migration. A similar rescue of migration was observed with specific ROCK inhibitors, H-1152 and H-1100 (see Fig. S3A to D in the supplemental material). The mechanism by which c-*jun* deletion and reduction in SCF leads to altered responsiveness to ROCK inhibitors remains to be determined.

Imatinib (Gleevec) is a small-molecule inhibitor of signaling by SCF through c-Kit, in addition to blocking Abl and platelet-derived growth factor signaling. As SCF promotes tumor cell proliferation and angiogenesis and c-Jun is frequently overexpressed in a broad array of human tumors, SCF inhibitors may thus provide adjunctive value in c-*jun*-expressing tumors. Given the important role of c-Jun as a bona fide oncogene (13, 23) and the common finding of c-Jun overexpression in tumors, it will be important to assess further the relative importance of SCF secretion mediated by c-Jun in regulating tumor metastases.

ACKNOWLEDGMENTS

We thank M. Karin for plasmids and helpful advice. Figure 11E was designed by Chenguang Wang.

This work was supported in part by R01CA70896, R01CA75503, R01CA86072, R01CA86071 (R.G.P.). The Kimmel Cancer Center was supported by an NIH Cancer Center Core grant P30CA56036 (R.G.P). This project is funded in part from the Ralph and Marian C. Falk Medical Research Trust and a grant from Pennsylvania Department of Health (R.G.P.).

The Pennsylvania Department of Health specifically disclaims responsibility for analyses, interpretations, or conclusions.

REFERENCES

1. **Albanese, C., M. D'Amico, A. T. Reutens, M. Fu, G. Watanabe, R. J. Lee, R. N. Kitsis, B. Henglein, M. Avantaggiati, K. Somasundaram, B. Thimmapaya, and R. G. Pestell.** 1999. Activation of the *cyclin D1* gene by the E1A-associated protein p300 through AP-1 inhibits cellular apoptosis. J. Biol. Chem. **274:**34186–34195.
2. **Albanese, C., J. Johnson, G. Watanabe, N. Eklund, D. Vu, A. Arnold, and R. G. Pestell.** 1995. Transforming p21^{ras} mutants and c-Ets-2 activate the cyclin D1 promoter through distinguishable regions. J. Biol. Chem. **270:** 23589–23597.
3. **Albanese, C., K. Wu, M. D'Amico, C. Jarrett, D. Joyce, J. Hughes, J. Hulit, T. Sakamaki, M. Fu, A. Ben-Ze'ev, J. F. Bromberg, C. Lamberti, U. Verma, R. B. Gaynor, S. W. Byers, and R. G. Pestell.** 2003. IKKα Regulates mitogenic signaling through transcriptional induction of cyclin D1 via Tcf. Mol. Biol. Cell **14:**585–599.
4. **Angel, P., and A. Szabowski.** 2002. Function of AP-1 target genes in mesenchymal-epithelial cross-talk in skin. Biochem. Pharmacol. **64:**949–956.
5. **Angel, P., A. Szabowski, and M. Schorpp-Kistner.** 2001. Function and regulation of AP-1 subunits in skin physiology and pathology. Oncogene **20:** 2413–2423.
6. **Bennett, B. L., D. T. Sasaki, B. W. Murray, E. C. O'Leary, S. T. Sakata, W. Xu, J. C. Leisten, A. Motiwala, S. Pierce, Y. Satoh, S. S. Bhagwat, A. M. Manning, and D. W. Anderson.** 2001. SP600125, an anthrapyrazolone inhibitor of Jun N-terminal kinase. Proc. Natl. Acad. Sci. USA **98:**13681–13686.
7. **Bouras, T., M. Fu, A. A. Sauve, F. Wang, A. A. Quong, N. D. Perkins, R. T. Hay, W. Gu, and R. G. Pestell.** 2005. SIRT1 deacetylation and repression of P300 involves lysine residues 1020/1024 within the cell-cycle regulatory domain 1. J. Biol. Chem. **280:**10264–10276.
8. **Burgess, A. W., H. S. Cho, C. Eigenbrot, K. M. Ferguson, T. P. Garrett, D. J. Leahy, M. A. Lemmon, M. X. Sliwkowski, C. W. Ward, and S. Yokoyama.** 2003. An open-and-shut case? Recent insights into the activation of EGF/ErbB receptors. Mol. Cell **12:**541–552.
9. **Coffer, P. J., N. Geijsen, L. M'Rabet, R. C. Schweizer, T. Maikoe, J. A. Raaijmakers, J. W. Lammers, and L. Koenderman.** 1998. Comparison of the roles of mitogen-activated protein kinase kinase and phosphatidylinositol 3-kinase signal transduction in neutrophil effector function. Biochem. J. **329:**121–130.

10. **D'Abaco, G. M., S. Hooper, H. Paterson, and C. J. Marshall.** 2002. Loss of Rb overrides the requirement for ERK activity for cell proliferation. J. Cell Sci. **115:**4607–4616.
11. **de Caestecker, M.** 2004. The transforming growth factor-beta superfamily of receptors. Cytokine Growth Factor Rev. **15:**1–11.
12. **Eferl, R., M. Sibilia, F. Hilberg, A. Fuchsbichler, I. Kufferath, B. Guertl, R. Zenz, E. F. Wagner, and K. Zatloukal.** 1999. Functions of c-Jun in liver and heart development. J. Cell Biol. **145:**1049–1061.
13. **Eferl, R., and E. F. Wagner.** 2003. AP-1: a double-edged sword in tumorigenesis. Nat Rev. Cancer **3:**859–868.
14. **Fu, M., C. Wang, M. Rao, X. Wu, T. Bouras, X. Zhang, Z. Li, X. Jiao, J. Yang, A. Li, N. D. Perkins, B. Thimmapaya, A. L. Kung, A. Munoz, A. Giordano, M. P. Lisanti, and R. G. Pestell.** 2005. Cyclin D1 represses p300 transactivation through a CDK-independent mechanism. J. Biol. Chem. **28:** 29728–29742.
15. **Galli, S. J., K. M. Zsebo, and E. N. Geissler.** 1994. The kit ligand, stem cell factor. Adv. Immunol. **55:**1–96.
16. **Gangnuss, S., A. J. Cowin, I. S. Daehn, N. Hatzirodos, J. A. Rothnagel, A. Varelias, and T. E. Rayner.** 2004. Regulation of MAPK activation, AP-1 transcription factor expression and keratinocyte differentiation in wounded fetal skin. J. Investig. Dermatol. **122:**791–804.
17. **Glise, B., and S. Noselli.** 1997. Coupling of Jun amino-terminal kinase and Decapentaplegic signaling pathways in *Drosophila* morphogenesis. Genes Dev. **11:**1738–1747.
18. **Gu, J., M. Tamura, R. Pankov, E. H. Danen, T. Takino, K. Matsumoto, and K. M. Yamada.** 1999. Shc and FAK differentially regulate cell motility and directionality modulated by PTEN. J. Cell Biol. **146:**389–403.
19. **Heinrich, M. C., C. D. Blanke, B. J. Druker, and C. L. Corless.** 2002. Inhibition of KIT tyrosine kinase activity: a novel molecular approach to the treatment of KIT-positive malignancies. J. Clin. Oncol. **20:**1692–1703.
20. **Hong, T., and L. B. Grabel.** 2006. Migration of F9 parietal endoderm cells is regulated by the ERK pathway. J. Cell. Biochem. **97:**1339–1349.
21. **Huang, C., K. Jacobson, and M. D. Schaller.** 2004. MAP kinases and cell migration. J. Cell Sci. **117:**4619–4628.
22. **Hulit, J., C. Wang, Z. Li, C. Albanese, M. Rao, D. Di Vizio, S. Shah, S. W. Byers, R. Mahmood, L. H. Augenlicht, R. Russell, and R. G. Pestell.** 2004. Cyclin D1 genetic heterozygosity regulates colonic epithelial cell differentiation and tumor number in Apc^{Min} mice. Mol. Cell. Biol. **24:**7598–7611.
23. **Karin, M., Z. Liu, and E. Zandi.** 1997. AP-1 function and regulation. Curr. Opin. Cell Biol. **9:**240–246.
24. **Klemke, R. L., S. Cai, A. L. Giannini, P. J. Gallagher, P. de Lanerolle, and D. A. Cheresh.** 1997. Regulation of cell motility by mitogen-activated protein kinase. J. Cell Biol. **137:**481–492.
25. **Krystal, G. W., S. J. Hines, and C. P. Organ.** 1996. Autocrine growth of small cell lung cancer mediated by coexpression of c-Kit and stem cell factor. Cancer Res. **56:**370–376.
26. **Kuan, C. Y., D. D. Yang, D. R. Samanta Roy, R. J. Davis, P. Rakic, and R. A. Flavell.** 1999. The Jnk1 and Jnk2 protein kinases are required for regional specific apoptosis during early brain development. Neuron **22:**667–676.
27. **Kumar, S., P. C. McDonnell, R. J. Gum, A. T. Hand, J. C. Lee, and P. R. Young.** 1997. Novel homologues of CSBP/p38 MAP kinase: activation, substrate specificity and sensitivity to inhibition by pyridinyl imidazoles. Biochem. Biophys. Res. Commun. **235:**533–538.
28. **Kyriakis, J. M.** 1999. Signaling by the germinal center kinase family of protein kinases. J. Biol. Chem. **274:**5259–5262.
29. **Lauffenburger, D. A., and A. F. Horwitz.** 1996. Cell migration: a physically integrated molecular process. Cell **84:**359–369.
30. **Li, G., C. Gustafson-Brown, S. K. Hanks, K. Nason, J. M. Arbeit, K. Pogliano, R. M. Wisdom, and R. S. Johnson.** 2003. c-Jun is essential for organization of the epidermal leading edge. Dev. Cell **4:**865–877.
31. **Li, Z., X. Jiao, C. Wang, X. Ju, Y. Lu, M. Lisanti, S. Katiyar, and R. G. Pestell.** 2006. Cyclin D1 induction of cellular migration requires $p27^{KIP1}$. Cancer Res. **66:**9986–9994.
32. **Li, Z., C. Wang, X. Jiao, Y. Lu, M. Fu, A. A. Quong, C. Dye, J. Yang, M. Dai, X. Ju, X. Zhang, A. Li, P. Burbelo, E. R. Stanley, and R. G. Pestell.** 2006. Cyclin D1 regulates cellular migration through the inhibition of thrombospondin 1 and ROCK signaling. Mol. Cell. Biol. **26:**4240–4256.
33. **Matsui, J., T. Wakabayashi, M. Asada, K. Yoshimatsu, and M. Okada.** 2004. Stem cell factor/c-kit signaling promotes the survival, migration, and capillary tube formation of human umbilical vein endothelial cells. J. Biol. Chem. **279:**18600–18607.
34. **Mitchison, T. J., and L. P. Cramer.** 1996. Actin-based cell motility and cell locomotion. Cell **84:**371–379.
35. **Neumeister, P., F. J. Pixley, Y. Xiong, H. Xie, K. Wu, A. Ashton, M. Cammer, A. Chan, M. Symons, E. R. Stanley, and R. G. Pestell.** 2006. Cyclin D1 governs adhesion and motility of macrophages. Mol. Biol. Cell **14:**2005–2015.
36. **Nobes, C. D., and A. Hall.** 1995. Rho, Rac, and Cdc42 GTPases regulate the assembly of multimolecular focal complexes associated with actin stress fibers, lamellipodia, and filopodia. Cell **81:**53–62.
37. **Noselli, S., and F. Agnes.** 1999. Roles of the JNK signaling pathway in *Drosophila* morphogenesis. Curr. Opin. Genet. Dev. **9:**466–472.
38. **Palmqvist, L., C. H. Glover, L. Hsu, M. Lu, B. Bossen, J. M. Piret, R. K. Humphries, and C. D. Helgason.** 2005. Correlation of murine embryonic stem cell gene expression profiles with functional measures of pluripotency. Stem Cells **23:**663–680.
39. **Pestell, R. G., and J. L. Jameson.** 1995. Hormone action II: transcriptional regulation of endocrine genes by second messenger signalling pathways, p. 59–76. *In* Bruce Weintraub (ed.), Molecular endocrinology: basic concepts and clinical correlations. Raven Press, New York, NY.
40. **Pritchard, C. A., L. Hayes, L. Wojnowski, A. Zimmer, R. M. Marais, and J. C. Norman.** 2004. B-Raf acts via the ROCKII/LIMK/cofilin pathway to maintain actin stress fibers in fibroblasts. Mol. Cell. Biol. **24:**5937–5952.
41. **Raivich, G., M. Bohatschek, C. Da Costa, O. Iwata, M. Galiano, M. Hristova, A. S. Nateri, M. Makwana, L. Riera-Sans, D. P. Wolfer, H. P. Lipp, A. Aguzzi, E. F. Wagner, and A. Behrens.** 2004. The AP-1 transcription factor c-Jun is required for efficient axonal regeneration. Neuron **43:**57–67.
42. **Ridley, A. J.** 2001. Rho GTPases and cell migration. J. Cell Sci. **114:**2713–2722.
43. **Rottner, K., A. Hall, and J. V. Small.** 1999. Interplay between Rac and Rho in the control of substrate contact dynamics. Curr. Biol. **9:**640–648.
44. **Sabeh, F., I. Ota, K. Holmbeck, H. Irkedal-Hansen, P. Soloway, M. Balbin, C. Lopez-Otin, S. Shapiro, M. Inada, S. Krane, E. Allen, D. Chung, and S. J. Weiss.** 2004. Tumor cell traffic through the extracellular matrix is controlled by the membrane-anchored collagenase MT1-MMP. J. Biol. Chem. **167:**769–781.
45. **Sage, J., A. L. Miller, P. A. Perez-Mancera, J. M. Wysocki, and T. Jacks.** 2003. Acute mutation of retinoblastoma gene function is sufficient for cell cycle re-entry. Nature **424:**223–228.
46. **Sander, E. E., S. van Delft, J. P. ten Klooster, T. Reid, R. A. van der Kammen, F. Michiels, and J. G. Collard.** 1998. Matrix-dependent Tiam1/Rac signaling in epithelial cells promotes either cell-cell adhesion or cell migration and is regulated by phosphatidylinositol 3-kinase. J. Cell Biol. **143:**1385–1398.
47. **Sasaki, Y., M. Suzuki, and H. Hidaka.** 2002. The novel and specific Rho-kinase inhibitor (S)-(+)-2-methyl-1-[(4-methyl-5-isoquinoline)sulfonyl]-homopiperazine as a probing molecule for Rho-kinase-involved pathway. Pharmacol. Ther. **93:**225–232.
48. **Shaw, L. M., I. Rabinovitz, H. H. Wang, A. Toker, and A. M. Mercurio.** 1997. Activation of phosphoinositide 3-OH kinase by the $\alpha 6\beta 4$ integrin promotes carcinoma invasion. Cell **91:**949–960.
49. **Shimokawa, H., M. Seto, N. Katsumata, M. Amano, T. Kozai, T. Yamawaki, K. Kuwata, T. Kandabashi, K. Egashira, I. Ikegaki, T. Asano, K. Kaibuchi, and A. Takeshita.** 1999. Rho-kinase-mediated pathway induces enhanced myosin light chain phosphorylations in a swine model of coronary artery spasm. Cardiovasc. Res. **43:**1029–1039.
50. **Shirai, K., Y. Okada, S. Saika, E. Senba, and Y. Ohnishi.** 2001. Expression of transcription factor AP-1 in rat lens epithelial cells during wound repair. Exp. Eye Res. **73:**461–468.
51. **Sibilia, M., and E. F. Wagner.** 1995. Strain-dependent epithelial defects in mice lacking the EGF receptor. Science **269:**234–238.
52. **Sluss, H. K., and R. J. Davis.** 1997. Embryonic morphogenesis signaling pathway mediated by JNK targets the transcription factor JUN and the TGF-beta homologue decapentaplegic. J. Cell Biochem. **67:**1–12.
53. **Sonnenberg, J. L., F. J. I. Rauscher, J. I. Morgan, and T. Curran.** 1989. Regulation of proenkephalin by Fos and Jun. Science **246:**1622–1625.
54. **Sugimoto, Y., T. Koji, and S. Miyoshi.** 1999. Modification of expression of stem cell factor by various cytokines. J. Cell Physiol. **181:**285–294.
55. **Sun, L., A. M. Hui, Q. Su, A. Vortmeyer, Y. Kotliarov, S. Pastorino, A. Passaniti, J. Menon, J. Walling, R. Bailey, M. Rosenblum, T. Mikkelsen, and H. A. Fine.** 2006. Neuronal and glioma-derived stem cell factor induces angiogenesis within the brain. Cancer Cell **9:**287–300.
56. **Szabowski, A., N. Maas-Szabowski, S. Andrecht, A. Kolbus, M. Schorpp-Kistner, N. E. Fusenig, and P. Angel.** 2000. c-Jun and JunB antagonistically control cytokine-regulated mesenchymal-epidermal interaction in skin. Cell **103:**745–755.
57. **Threadgill, D. W., A. A. Dlugosz, L. A. Hansen, T. Tennenbaum, U. Lichti, D. Yee, C. LaMantia, T. Mourton, K. Herrup, R. C. Harris, et al.** 1995. Targeted disruption of mouse EGF receptor: effect of genetic background on mutant phenotype. Science **269:**230–234.
58. **Thumkeo, D., Y. Shimizu, S. Sakamoto, S. Yamada, and S. Narumiya.** 2005. ROCK-I and ROCK-II cooperatively regulate closure of eyelid and ventral body wall in mouse embryo. Genes Cells **10:**825–834.
59. **Toda, M., M. Dawson, T. Nakamura, P. M. Munro, R. M. Richardson, M. Bailly, and S. J. Ono.** 2004. Impact of engagement of FcεRI and CC chemokine receptor 1 on mast cell activation and motility. J. Biol. Chem. **279:**48443–48448.
60. **Todaro, G. J., and H. Green.** 1963. Quantitative studies of the growth of mouse embryo cells in culture and their development into established lines. J. Cell Biol. **17:**299–313.
61. **Vassalli, A., M. M. Matzuk, H. A. Gardner, K. F. Lee, and R. Jaenisch.** 1994. Activin/inhibin beta B subunit gene disruption leads to defects in eyelid development and female reproduction. Genes Dev. **8:**414–427.
62. **Ventura, J. J., N. J. Kennedy, R. A. Flavell, and R. J. Davis.** 2004. JNK regulates autocrine expression of TGF-beta1. Mol. Cell **15:**269–278.

63. **Vleugel, M. M., A. E. Greijer, R. Bos, E. van der Wall, and P. J. van Diest.** 2006. c-Jun activation is associated with proliferation and angiogenesis in invasive breast cancer. Hum. Pathol. **37:**668–674.
64. **Walters, R. W., T. Grunst, J. M. Bergelson, R. W. Finberg, M. J. Welsh, and J. Zabner.** 1999. Basolateral localization of fiber receptors limits adenovirus infection from the apical surface of airway epithelia. J. Biol. Chem. **274:** 10219–10226.
65. **Wang, C., N. Pattabiraman, M. Fu, J. N. Zhou, T. Sakamaki, C. Albanese, Z. Li, K. Wu, J. Hulit, P. Neumeister, P. M. Novikoff, M. Brownlee, P. Scherer, J. G. Jones, K. D. Whitney, L. A. Donehower, E. L. Harris, T. Rohan, D. C. Johns, and R. G. Pestell.** 2003. Cyclin D1 repression of peroxisome proliferator-activated receptor γ expression and transactivation. Mol. Cell. Biol. **23:**6159–6173.
66. **Wang, P., M. Anton, F. L. Graham, and S. Bacchetti.** 1995. High frequency recombination between loxP sites in human chromosomes mediated by an adenovirus vector expressing Cre recombinase. Somat. Cell Mol. Genet. **21:**429–441.
67. **Weber, J. D., D. M. Raben, P. J. Phillips, and J. J. Baldassare.** 1997. Sustained activation of extracellular-signal-regulated kinase 1 (ERK1) is required for the continued expression of cyclin D1 in G1 phase. Biochem. J. **326:**61–68.
68. **Xia, Y., and M. Karin.** 2004. The control of cell motility and epithelial morphogenesis by Jun kinases. Trends Cell Biol. **14:**94–101.
69. **Xia, Z., M. Dickens, J. Raingeaud, R. J. Davis, and M. E. Greenberg.** 1995. Opposing effects of ERK and JNK-p38 MAP kinases on apoptosis. Science **270:**1326–1331.
70. **Yarden, Y., W. J. Kuang, T. Yang-Feng, L. Coussens, S. Munemitsu, T. J. Dull, E. Chen, J. Schlessinger, U. Francke, and A. Ullrich.** 1987. Human proto-oncogene c-kit: a new cell surface receptor tyrosine kinase for an unidentified ligand. EMBO J. **6:**3341–3351.
71. **Zenz, R., H. Scheuch, P. Martin, C. Frank, R. Eferl, L. Kenner, M. Sibilia, and E. F. Wagner.** 2003. c-Jun regulates eyelid closure and skin tumor development through EGFR signaling. Dev. Cell **4:**879–889.
72. **Zhang, L., W. Wang, Y. Hayashi, J. V. Jester, D. E. Birk, M. Gao, C. Y. Liu, W. W. Kao, M. Karin, and Y. Xia.** 2003. A role for MEK kinase 1 in TGF-beta/activin-induced epithelium movement and embryonic eyelid closure. EMBO J. **22:**4443–4454.
73. **Zhang, Z., R. Zhang, A. Joachimiak, J. Schlessinger, and X. P. Kong.** 2000. Crystal structure of human stem cell factor: implication for stem cell factor receptor dimerization and activation. Proc. Natl. Acad. Sci. USA **97:**7732–7737.
74. **Zsebo, K. M., D. A. Williams, E. N. Geissler, V. C. Broudy, F. H. Martin, H. L. Atkins, R. Y. Hsu, N. C. Birkett, K. H. Okino, D. C. Murdock, and et al.** 1990. Stem cell factor is encoded at the Sl locus of the mouse and is the ligand for the c-kit tyrosine kinase receptor. Cell **63:**213–224.